Diyala Journal for Pure Science

Deposition of Iron Oxide Thin Films by Spray Pyrolysis Method

Sanaa Rafat Yaseen

Medical Laboratory Technical department – Erbil Health and Medical Technical College, Erbil Polytechnic University, Erbil, Iraq

sanaa.rafat@yahoo.com

Received: 25 April 2022 **Accepted: 27 June 2022**

DOI: https://dx.doi.org/10.24237/djps.1803.579A

Abstract

The growth and characterization of iron oxide thin films by spray pyrolysis method using iron chloride hexahydrate. Iron oxide films deposited on well cleaned glass substrate at different substrate temperatures varying from 250^{0}C to 500^{0}C in air atmosphere. The characterization of iron oxides films was investigated for their optical and morphological properties by using spectroscopy and Scanning Electron Microscopy. The atomic absorption spectroscopy showed the existence of direct band gap energy nearly 2.18 eV with varying substrate temperature. Optical, structural and morphological observations were showed the film quality was getting better at 350 ^{0}C substrate temperature, also grain sizes were cleared.

Keywords: Fe_2O_3 films, X-ray diffraction, Optical absorption.

Diyala Journal for Pure Science

Deposition of (Iron Oxide) Thin Films by Spray Pyrolysis Method

Sanaa Rafat Yaseen

ترسب الأفلام الرقيقة (أكسيد الحديد) عن طريق رذاذ الانحلال الحراري باستخدام مركبات فيروم مختلفة

سناء رفعت ياسين

قسم تقنيات المختبرات الطبية – كلية أربيل للصحة التقنية – جامعة أربيل التقنية

الخلاصة

أودعت هذه الدراسة أفلام أكسيد الحديد عن طريق رذاذ الانحلال الحراري في ظل ظروف ترسب مختلفة. تم التحقيق في تأثير تقنية التحضير على الخصائص الهيكلية والبصرية لأفلام Fe2O3 أكسيد الحديد باستخدام حيود الأشعة السينية (XRD). تم إعداد أفلام أكسيد الحديد Fe2O3 عن طريق تقنية الانحلال الحراري الرش في درجات حرارة الركيزة المختلفة، وذلك باستخدام FeCl3.6H2O، FeCl3.4H2O ، و FeSO4.7H2O (0.1M). ودرست بنية الكريستال من الأفلام من قبل حيود الأشعة السينية كما درس أن هناك قمم الحيود موجودة مع قيم 38.5232 ;a، 44.77، 65.16، 78.297 في درجات، المقابلة للطائرات الكريستال من (320)، (410)، (200)، (444) من أكسيد الحديد البلوري والحديد لكل درجة حرارة الركيزة، على التوالي. جميع الأفلام درجة حرارة الركيزة تظهر نفس الهياكل الكريستال. يتغير مستوى البلورة وفقا لدرجة حرارة الركيزة؛ وقد لوحظ أفضل بلورة في درجة حرارة الركيزة 350 درجة مئوية. أفلام أكسيد الحديد رش المودعة في الركيزة.

كلمات مفتاحية: أفلام Fe2O3، فيلم رقيق، رذاذ الانحلال الحراري

Diyala Journal for Pure Science

Deposition of (Iron Oxide) Thin Films by Spray Pyrolysis Method

Sanaa Rafat Yaseen

Introduction

Iron oxides are employed in various activities, including material science, soil science, industrial chemistry, medicine, chemistry, and corrosion science. This is due to the fascinating magnetic characteristics, crystal shapes, and different compositions of these materials. When it comes to iron, there are three types of iron oxides that may be found in the Earth's crust: hematite (α-Fe_2O_3), maghemite (γ-Fe_2O_3) and magnetite (Fe_3O_4) [1]. Iron oxides are often used in cosmetics to create wall murals and aesthetic adornment for colours [2]. As a result of advances in nanotechnology, a wide range of new applications have emerged [3]. These particles have acceptable magnetic characteristics, minimal cytotoxicity, biodegradability, biocompatibility, chemical stability, decreased particle size, and high surface area [4].

Thermal barriers, corrosion prevention, and optical applications all benefit from the versatility and low cost of thin films. Spray pyrolysis, chemical vapor deposition, chemical bath deposition, pulsed laser deposition, and electron beam deposition are some of the deposition methods available. For thin films, spray pyrolysis is the most straightforward method. Because it's a coating procedure that yields a variety of useful goods, the instrument is simple to use and inexpensive to purchase. Pyrolysis of the substrates results in nearly oxide layers on the substrate surface that are excellently homogenous. The component of the precursor solution is the single factor that determines the attention combination of the deposited layers [5].

Spray pyrolysis is a process for creating thin films, coatings, and dust using high temperatures and high pressures. If you compare spray pyrolysis to other techniques that involve costly materials and laborious processes, spray pyrolysis is the most advantageous option. It allows for the easy production of films using everyday items. The use of porous films and massive quantities of substrates or chemicals is not necessary [6].

Deposition of (Iron Oxide) Thin Films by Spray Pyrolysis Method

Sanaa Rafat Yaseen

The main purpose of this study is to investigate the role of Ferrum compounds on the structural and optical properties of iron oxide films and to obtain the optimum experimental conditions for the best quality.

Material and Methods

Traditional and versatile spraying methods may be used to produce metal oxide films, and the substrate temperature is necessary.

Film preparation

A 0.01 molar of $FeCl_3.6H_2O$ was used to prepare the thin films of iron oxides α-Fe_2O_3, in 50 ml of distilled water. The glass substrates were preheated and then later sprayed for 10s with the obtained clear yellow solution. Prior to that, the solution went through a 0.7 mm nozzle diameter of a pneumatic nebulizer. In order to prevent the glass substrates from excessive cooling, attention was made to ensure that a 5-minutes time span was allocated between each spraying process. The film preparation process to determine the effects of changes in the substrate temperature from 250, 300, 350, 400, 450 to 500 ˚C. If the thin-film production is successful, the substrates need to be well cleaned and prepared before to application. The cleaning process ensures that the substrates do not have any contaminants and remain clean. A UV/VIS spectrophotometer is used to calculate the thin film's optical absorption of spray pyrolysis on a glass substrate which is performed at a wavelength ranging between 300 nm and 900 nm. This involves measuring the intensity and dilution of the mean between the source and the detector

Diyala Journal for Pure Science

Results and Discussion

Structural, Compositional and Optical Analysis of Iron Oxide Films

XRD is supported by Bragg's Law. Mathematically, Bragg's Law is as follows:

$$n\lambda=2d\sin\theta \quad (1)$$

d is the distance between crystalline planes, θ is the Bragg angle from which the X-ray diffracted, and λ is the wavelength of the X-ray. Crystal lattice spacing affects the angle at which incident X-rays are diffracted. Peak Positions in the diffraction pattern provide information on the size and shape of the unit cell, whereas Peak Intensities provide information on the density of electrons inside the unit cell, i.e. the locations of atoms. It is possible to determine the pattern by looking at the Miller indices (hkl) for each peak. Inter-planar spacing dhkl may be estimated using Bragg's relation from XRD patterns for (hkl) plane.

In order to establish the preferred crystal orientation of the sprayed iron oxide coatings, XRD analysis was used. Comparing 2 θ values and intensities helped identify the crystal phases. It is clear from the diffraction pattern that the films' crystal structure is polycrystalline.

Experiments using $FeCl_3.6H_2O$ yielded the following results: Table 1 lists the FWHM, peak height and interplanar spacing d for each film deposited from solution. The longest inter-planar spacing d=2.3425 at substrate temperature 400 ºC is determined by the first major peak of each sample, and the smallest peak height for the first peak is determined by d=776.3 at the smallest peak height of d=776.3. In Table 1, we see the FWHM values of substrate temperatures at 250 ºC, 350 ºC, 400 °C, and 450 °C. The X-ray diffraction pattern was used to examine the crystallinity of iron oxide films. For each peak, the 2 value of each peak was examined from the XRD pattern and hkl values (hkl) from literature and JCPDS data were used to determine the Miller indices (hkl). When iron oxide films are sprayed at various substrate temperatures, the pattern doesn't differ significantly from one another. For each substrate temperature, the same four major peaks could be found.

Deposition of (Iron Oxide) Thin Films by Spray Pyrolysis Method

Sanaa Rafat Yaseen

Table 1: Measured XRD results for $FeCl_3.6H_2O$

SUBSTRATE TEMPERATURE (^OC)	2Θ (DEG)	PEAK HEIGHT	FWHM (RADIAN)	INTER-PLANAR SPACING D (Å)
250	38.523	907.7	0.1312	2.3370
	44.77	946.3	0.2623	2.0242
	65.16	1000	0.1312	1.4317
	78.297	654.5	0.1312	1.2211
300	38.476	1000	0.1128	2.3398
	44.718	467	0.1658	2.0266
	65.093	442.6	0.2661	1.4330
	78.225	304.4	0.3252	1.2221
350	38.46	1000	0.2623	2.3405
	44.71	656.3	0.1312	2.0272
	65.08	888.9	0.1312	1.4330
	78.22	552.5	0.1312	1.2220
400	38.43	776.3	0.2623	2.3425
	44.69	1000	0.2623	2.0278
	65.08	638.8	0.1312	1.4333
	78.20	540.4	0.1312	1.2224
450	38.46	877	0.2623	2.3409
	44.71	1000	0.2623	2.0271
	65.09	962.1	0.1312	1.4331
	78.225	649.3	0.1312	1.2221
500	38.466	1000	0.1217	2.3404
	44.697	555.4	0.1408	2.0275
	65.032	711.3	0.1232	1.4342
	78.157	508.7	0.1510	1.2230

In this case, d is the lattice constant, and hkl is a miller index. The lattice constant 'a' is confirmed to be the same orientation in (320) and (410) based on the results of these calculations. Fe_3O_4 is the most common source of γ-Fe_2O_3. For γ-Fe_2O_3 (0.83474 Å), the lattice parameter is a tad smaller than Fe_3O_4's (0.8396 Å).

Diyala Journal for Pure Science

Deposition of (Iron Oxide) Thin Films by Spray Pyrolysis Method

Sanaa Rafat Yaseen

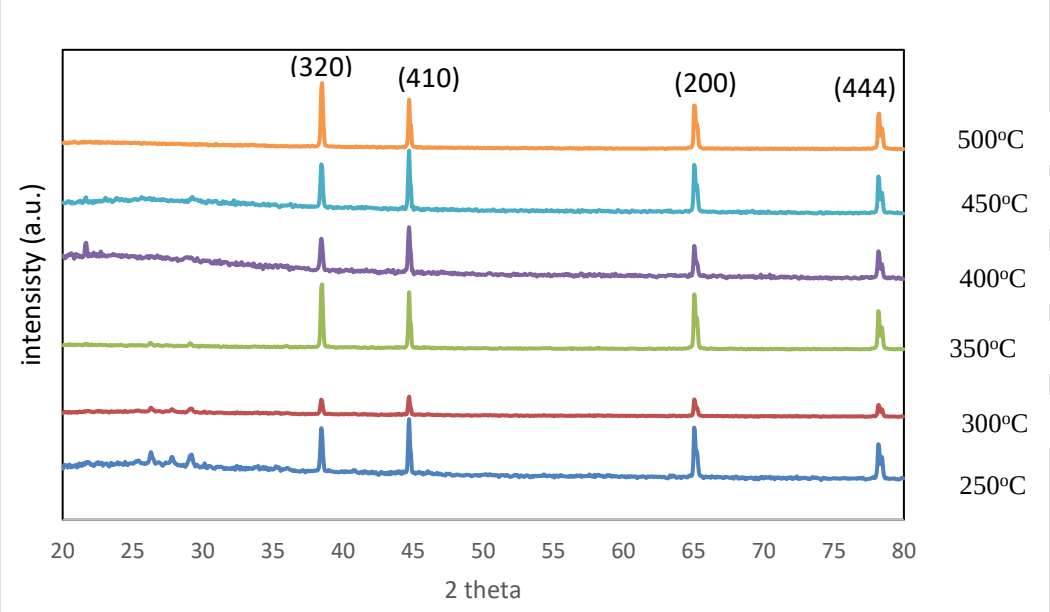

Figure 1: XRD Patterns for the Fe_2O_3 films prepared using $FeCl_3.6H_2O$.

It was confirmed by the calculated lattice constants (a=8.42Å) and (a=8.35Å) that the first two peaks had plane orientations consistent with the lattice. The calculated lattice constant a=2.87Å confirms the presence of metallic -iron in the third peak (BCC). Iron crystalline fourth peaks (444) and (622) have lattice constants of 8.42 Å and 8.09Å, respectively, according to the literature, which shows two different plane orientations. According to these findings, the (444) iron crystalline orientation can be confirmed by the two theta values (78-78.297) of the fourth peak at a lattice constant (a=8.12Å). At any substrate temperature, the diffraction peaks are not shifted in any direction; all substrate temperature films exhibit the same crystal structures. (Fig.1) shows that the crystallinity level changes with substrate temperature; the best crystallinity was observed at 350 oC. According to this, the peak height of the film sprayed at substrate temperature 300 oC is the lowest showed diminishing crystallinity, which means that the crystalline defects are greatly increased for this substrate temperature. Decreasing Full width half maximum and increasing peak height indicate improving crystallinity level. For all sprayed iron oxides, the preferred direction trend is (320). The two theta values of diffracted

peaks are not significantly affected when the substrate temperature changes, but peak intensities are. Up to a substrate temperature of 350 oC, peak intensities increase. It was proof that crystallinity was rising. The iron oxides film was sprayed at 350 oC, and the XRD pattern was (Fig 2).

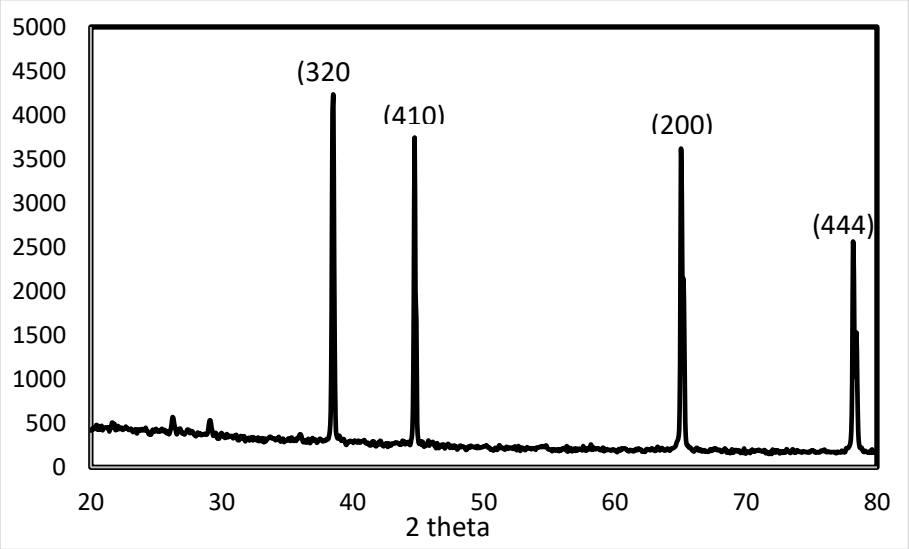

Figure 2: XRD pattern for iron oxide film sprayed at substrate temperature 350 °C for $FeCl_3.6H_2O$.

Although the crystallographic orientation cannot be determined by the XRD patterns, they can be used to determine the crystallite size (D), grain size, dislocation density, and strain.

The crystallite sizes of each sample were estimated by using the Debye-Scherrer formula;

$$\boldsymbol{D = \frac{0.94\lambda}{\beta \cos \theta}} \qquad \textbf{(2)}$$

The microstrain (Ɛ) value of the sprayed iron oxide films was calculated from equation (3):

$$\varepsilon = \frac{\beta \cos \theta}{4} \qquad \textbf{(3)}$$

Where β is the full width at half maximum (FWHM) of the diffraction peaks. Table 2 lists all estimated structural parameters, dislocation density, hkl values, grain size, FWHM, and strain.

Because of the inverse relationship between grain size and dislocation density, the dislocation density decreases with increasing crystallite size for the second peak oriented (410) at substrate temperature 350 ^{o}C, implying improved crystalline characteristics of films. The average XRD diffracts gram crystallite size ranged between 3349936.6 and 8150428.8 nm. Grain size increases are attributable to high crystallinity and shrinking grain boundaries. The rise in crystallinity is found to be directly proportional to the increase in grain size, the increase in diffraction peak intensities, and the narrowness of the full width half maximum.

Table 2: Structural parameters calculated for $FeCl_3.6H_2O$

Substrate temperature (C^o)	Peak 2 theta (2θ)	FWHM	Miller indices d_{hkl}	Grain size(nm)	Dislocation density ($\times 10^{-14}$)	Strain
250	38.502	0.1312	320	6698788.7	2.2285	0.0005404
250	44.74	0.2623	410	3420738.4	8.5459	0.0010583
250	65.16	0.1312	200	7505234.1	1.7753	0.0004823
250	78.297	0.1312	444	8154885.4	1.5037	0.0004439
300	38.476	0.1128	320	7790881.6	1.6475	0.0004647
300	44.718	0.1658	410	5411271.4	3.4151	0.0006690
300	65.093	0.2661	200	3699057.3	7.3083	0.0009787
300	78.225	0.3252	444	3288358.6	9.2479	0.0011009
350	38.46	0.2623	320	3350242.4	8.9094	0.0010806
350	44.63	0.1312	410	6838133.4	2.1386	0.0005294
350	65.08	0.1312	200	7501889.4	1.7769	0.0004826
350	78.22	0.1312	444	8150428.8	1.5054	0.0004442
400	38.43	0.2623	320	3349936.6	8.9111	0.0010807
400	44.63	0.2623	410	3419389.3	8.5527	0.0010587
400	65.08	0.1312	200	7501889.4	1.7769	0.0004826
400	78.2	0.1312	444	8149272.7	1.5058	0.0004442
450	38.46	0.2623	320	3350242.4	8.9094	0.0010806
450	44.71	0.2623	410	3420370.2	8.5478	0.0010584
450	65.032	0.1312	200	7502307.1	1.7767	0.0004825
450	78.22	0.1312	444	8150428.8	1.5054	0.0004442
500	38.466	0.1217	320	7220909.0	1.9179	0.0005013
500	44.697	0.1408	410	6371599.8	2.4632	0.0005682
500	65.032	0.1232	200	7986891.1	1.5676	0.0004532
500	78.157	0.1511	444	7078534.4	1.9958	0.0005114

Diyala Journal for Pure Science

The six SEM images are shown in Fig.3 below according to their deposition temperature.

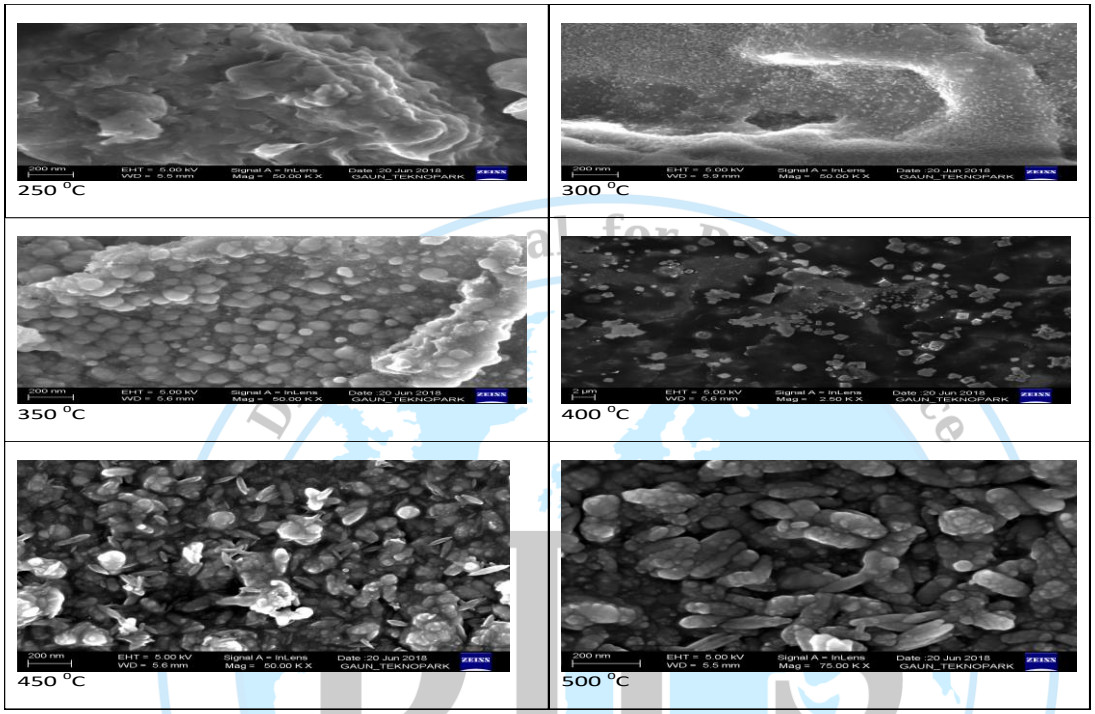

Figure 3: SEM images of the particles obtained from $FeCl_3.6H_2O$ solution by the different substrate temperatures of 250 ^{0}C, 300 ^{0}C,350 ^{0}C, 400 ^{0}C, 450 ^{0}C,500 ^{0}C.

SEM photographs demonstrate the improvement of crystallinity; the best crystal structure is identified from XRD patterns at substrate temperature 350 ^{o}C, and SEM images (Fig.3) show the same investigation. SEM scans clearly show grains at this temperature. It can be shown that increasing grain size and minimizing grain boundaries enhanced crystallinity. Energy Dispersive X-ray Analysis (EDX) is a popular technique for determining the chemical composition of an unknown material. The peaks in the EDX spectrum are detected using this technique, and each peak is unique for an atom that corresponds to a single element. Elemental studies are performed using the energy dispersive X-ray method; the existence of Fe and O elements can be seen by the presence of peaks corresponding to Fe and O elements. The elemental analysis was limited to Fe and O, confirming the creation of iron oxide.

These results are showed in the figures below for $FeCl_3.6H_2O$ solution (Fig.4)

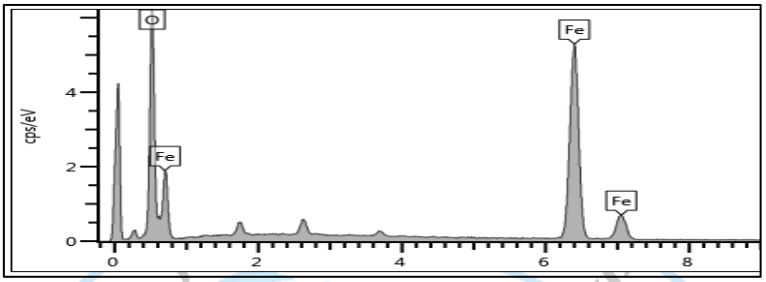

Figure 4: EDX spectrum of sprayed iron oxide film at substrate temperature 350ºC.

For each substrate temperature, the optical band gap of sprayed iron oxide films was calculated using UV-visible absorption spectroscopy. The optical band gap was calculated using the following formula (4):

$$\alpha = \frac{A(h\nu - E_g)^n}{h\nu} \quad (4)$$

where n=1/2 for direct transition and n=2 for indirect transition, α is the absorption coefficient, A is materials dependent constant, E_g Optical band gap. The usual method of obtaining optical band gap is plotting $(\alpha h\nu)^{1/n}$ versus $h\nu$ (Fig.5)

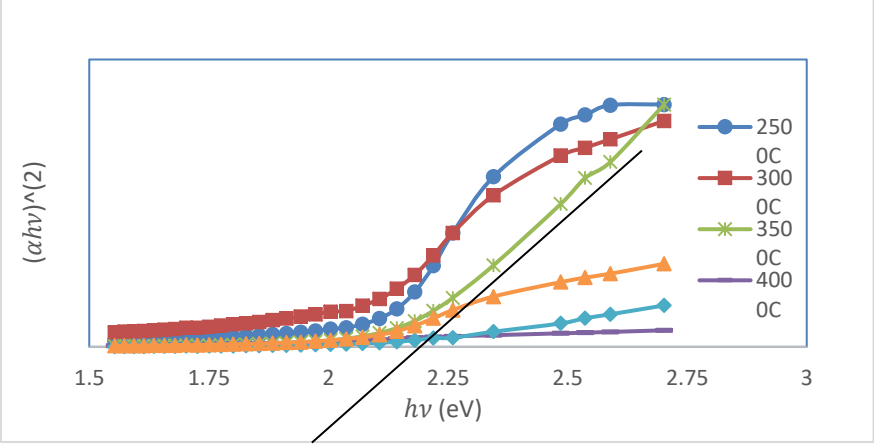

Figure 5: Variation of $(\alpha h\nu)^2$ with photon energy $h\nu$ for α-Fe_2O_3 films with different substrate temperatures.

Diyala Journal for Pure Science

Deposition of (Iron Oxide) Thin Films by Spray Pyrolysis Method

Sanaa Rafat Yaseen

The band gap values obtained for sprayed iron oxides in this work corresponded with previously reported values. The optical band gap was found to be 2.03, 2.04, 2.18, 1.75, 2.04 and 2.04 eV for varied substrate temperatures of 250 ^{o}C, 300 ^{o}C, 350 ^{o}C, 400 ^{o}C, 450 ^{o}C, and 500 ^{o}C. The sprayed iron oxide films produced at 350 ^{o}C substrate temperature had a greater bandgap of 2.18 eV, indicating an increase in crystallinity. The same conclusions were reached by XRD analysis; the best crystallinity was found for the substrate temperature of 350 ^{o}C. This demonstrates that sprayed iron oxide coatings with higher crystallinity also have a higher bandgap. (Fig.6) depicts the fluctuation of $(\alpha hv)^{\wedge 2}$ with photon energy h for α-Fe_2O_3 films at 350 ^{o}C substrate temperature.

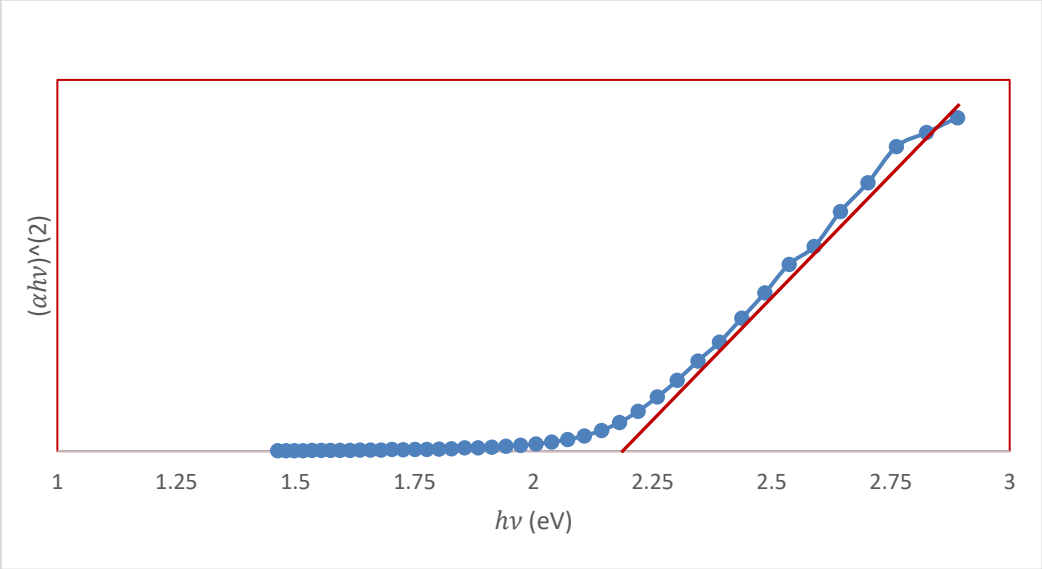

Figure 6: Variation of $(\alpha hv)^2$ with photon energy hv for α-Fe_2O_3 films at substrate temperature 350^0 C for $FeCl_3.6H_2O$.

The spray pyrolysis process is used to grow and characterize iron oxide layers. Optical and structural measurements revealed that the film quality was improving at 350 ^{o}C substrate temperature.

According to (7), Fe_2O_3 thin films were formed on quartz substrates employing ultrasonic spray pyrolysis at deposition temperatures ranging from 400 to 700 degrees Celsius. An ultrasonic nebulizer with an atomizing frequency of 1.67 MHz was used to atomize the chemical solution into the stream of fine droplets. From the intake side, the chloride precursor solution was poured into the vessel. The vibration of the transducer produced the aerosol. The hot substrate was applied with the nebulized spray that rises in the column. However, as previously said, we disagreed with our findings concerning XRD pattern outcomes; our preferred temperature is 350 ˚C.

The XRD patterns of iron oxide thin films produced by ultrasonic spray pyrolysis on quartz substrate at various deposition temperatures are shown in the results. The film formed on quartz at Ts =400 ^oC was found to be amorphous, but the film deposited at Ts =500 ^oC was found to be crystalline. The results reveal that increasing the substrate temperature promotes the diffusion of atoms absorbed on the substrate and speeds the migration of atoms to more energy-efficient places, resulting in increased crystallinity.

(8) demonstrated the energy band gap and optical transmittance spectra of Fe_2O_3 thin films in the preceding study (8). We used the Tauc's connection to determine the direct band gap. This study found similar results, and the optical band gap can be calculated by projecting the linear region to the energy axis. α - Fe_2O_3 films or nanoparticles can be generated by direct or indirect transition, as well as several other described methods (4, 9). The obtained direct band gap values in this study were quite close to the value provided by (10). And had a greater band gap than the film deposited at 500 ˚C, which could be attributable to an increase in crystallinity with increasing substrate temperature, which leads to fewer defects and a better crystal structure. Furthermore, as previously reported by, the predicted band gap for the Fe_2O_3 nanopowder was found to be about 2.5 eV. (11).

The present study used a chemical spray approach to deposit nickel-doped zinc oxide thin films (ZnO: Ni) at varied percentages (0–10%) on glass substrates. The influence of Ni concentration

on the structural and optical properties of ZnO: Ni thin films was studied. X-ray diffraction (XRD), UV–vis, Photoluminescence spectra PL, and Raman spectroscopy were used to evaluate the effect of Ni concentrations on the crystalline structure and optical properties of the films. The XRD investigation revealed that both the undoped and Ni-doped ZnO films formed in a hexagonal structure, with the crystallites preferentially oriented along the [002] direction perpendicular to the substrate. The XRD investigation further revealed that the films were well crystallized in the würtzite phase, with crystallites preferentially orientated parallel to the c-axis in the (002) direction. The optical analysis revealed that all of the films were extremely transparent. The bandgap dropped to 7 % Ni doping level, however it rose beyond ten percent Ni doping level. In the visible area, all thin films had transmittance of 80 % or above. The PL spectra of undoped and Ni-doped ZnO thin films revealed some distinct peaks at 376, 389, 494, and 515 nm. The obtained results demonstrated that doping levels had a significant impact on the structures and optical properties of the films. A work by (14) discovered the role of structural characteristics of crystallites by XRD and UV examination in different orientations, which contradicts our findings.

In another study by (13), they found quality crystal rather than we reported the electrochemical supercapacitor performance Hematite α-Fe_2O_3 thin films prepared by spray pyrolysis from a non-aqueous medium.

(12) investigated the crystalline quality of Fe2O3 thin films spray deposited at various temperatures using the same procedure as we did; X-ray diffraction (XRD) analysis was performed, and the findings are reported. The observed peaks at 2θ around 24.16°, 33.10°, 35.64°, 39.62°, 40.81°, 43.76°, 49.59°, 54.15°, 57.82°, 62.71°, and 64.25° can be assigned to Rhombohedral α-Fe2O3 (JCPDS card no. 84-0311) with the lattice planes of (012), (104), (110), (006), (113), (202), (024), (116), (122), (214), and (300), respectively. Films are shown to be strongly orientated along the (104) plane. Fe_2O_3 has a rhombichedral crystal structure, which was validated by comparing the computed and conventional "d" values. No other

substances like γ- Fe_2O_3, Fe_3O_4, or organic impurities were discovered. The peak (104) intensity was observed to be substrate temperature-dependent. Additionally, it has been found that the peak (104) intensity increases as substrate temperature rises, reaches a maximum value at 350 °C, and then falls. An improvement in the crystallinity of the Fe_2O_3 thin films is indicated by the increase in peak (104) intensity.

Conclusions

In this work, iron oxide thin films are deposited by spray pyrolysis method using ferrum compounds such as $FeCl_3.6H_2O$. The summary of this study is the investigation of the role of ferrum compounds on the structural, optical and morphological properties of iron oxide films. The sprayed solution was prepared by $FeCl_3.6H_2O$ (0.1M) and distilled water. Iron oxide films deposited on well cleaned glass substrate at different substrate temperatures varying from 250 ^oC to 500 ^oC in air atmosphere. Also, we couldn't cover the films we did with $FeCl_3.4H_2O$, so we haven't conducted any of these techniques by XRD, SEM, EDX results show that when the temperature it reaches 350 ^oC the film will be clear and it greater available in this temperature for the $FeCl_3.6H_2O$, we have band gap 2.18 eV. We have found that Fe_2O_3 thin film exhibit a polycrystalline having (320), (410), (200) and (444) plans of high peak intensities.

References

1. W. He, P. J. Liu, G. Q. He, M. Gozin, Q. L.Yan, Advanced Materials Oct, 30(41), 1706293(2018)
2. S. R. Yaseen, Characterization of iron oxide thin films deposition by spray pyrolysis using different ferrum compounds, Master's thesis, Fen Bilimleri Enstitüsü,(2019)
3. H. J. Ahmed, A. A . Kamil, A. A. Habeeb, N. A. Bakr, International Research Journal of Science and Technology, 1(2), 149-55(2020)

4. A. K. Bashir, N. Mayedwa, K. Kaviyarasu, L. C. Razanamahandry, N. Matinise, K. Bharuth-Ram, M. T. Tchokonté, F. I. Ezema, M. I. Maaza, Surfaces and Interfaces, 1(17), 100345(2019)

5. F. M. Tarmidzi, S. B. Sasongko, International Journal of Applied Engineering Research,13(12), 10234-9(2018)

6. I. J. Mbonu, C. C. Mbonu, Journal of the Indonesian Chemical Society, 31,3(2),87(2020)

7. F. Loghmani, N. Mirghaffari, M. Soleimani, Pollution, 1,5(4),775-88(2019)

8. P. Singh, A. Kaushal, D. Kaur, Journal of Alloys and Compounds, 471(1-2),11-5(2009)

9. V. K. Yadav, G. Gnanamoorthy, D. Ali, S. P. Bera, A. Roy, G. Kumar, N. Choudhary, H. Kalasariya, A. Basnet, Journal of Nanomaterials, (2022)

10. R. MS, Asian Journal of Applied Science and Technology (AJAST), 5(1),72-81(2021)

11. R. N. Goyal, A.K. Pandey, D. Kaur, A. Kumar, Journal of nanoscience and nanotechnology, 9(8),4692-9(2019)

12. V. K. Yadav, D. Ali, S.H. Khan, G. Gnanamoorthy, N. Choudhary, K. K. Yadav, V. N. Thai, S. A. Hussain, S. Manhrdas, Nanomaterials,10(8),1551(2020)

13. H. D. OMAR, Journal of Engineering Technology and Applied Sciences, 4(1),1-0(2019)

14. S. U. Khayam, M. Usman, M. A. Umer, A. Rafique, Materials & ,192,108748(2020)